

Evaluation of the Possibility of Upgrading the Advanced Photon Source to an Energy Recovery Linac^{*}

Michael Borland

*Argonne National Laboratory, 9700 South Cass Avenue, Argonne, IL, 60439 USA,
borland@aps.anl.gov*

Abstract

One of the concepts being explored for a next-generation x-ray source is the Energy Recovery Linac (ERL). It is well known that, as a synchrotron radiation source matures, the value of the x-ray beamlines and experimental infrastructure approaches and then exceeds the value of the accelerator complex. Hence, it makes sense to think of eventually upgrading the Advanced Photon Source (APS) to an ERL. We explore through simulation the potential performance that might be obtained by injecting an ERL beam into the APS and circulating one or more turns. Issues covered include lattice choices, coherent synchrotron radiation effects, bunch lengthening, and lattice options. We also give a comparison of the expected brightness to that of the present APS.

Key words: synchrotron radiation sources, beam dynamics, coherent synchrotron radiation

PACS: 29.20.-c, 29.27.-a, 29.27.Bd

1 Introduction

The Advanced Photon Source (APS) is a 7-GeV, third-generation synchrotron radiation facility supplying x-ray beams to approximately 50 experimental stations. Development of the remaining beamlines and build-up of experimental stations will continue into the foreseeable future, resulting in a complex, costly accumulation of facilities and equipment surrounding the APS ring. At

^{*} Work supported by the U.S. Department of Energy, Office of Basic Energy Sciences, under Contract No. W-31-109-ENG-38.

present, few APS users are truly limited by the available source properties. However, we expect this to change and that eventually the APS ring will need to be upgraded. One of the options we are exploring is a replacement storage ring with ultra-high brightness [1]. In this paper, we evaluate an alternative possibility for APS, namely injection of a high-brightness beam from a linear accelerator [2].

The concept under considerations is shown in Figure 1. We assume the existence of a high-brightness injector and superconducting linac. The beam from this system is injected into the APS and allowed to circulate one or more turns. The option of circulating several turns would perhaps provide a higher brightness source without the necessity of have a high duty factor injector. It may or may not require energy recovery, depending on how many turns can be utilized and how high an average current is required in the ring.

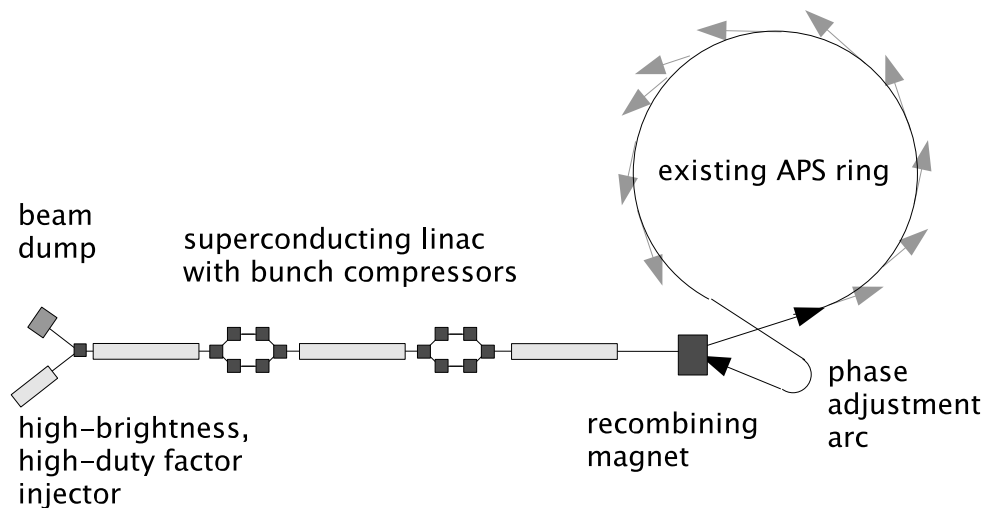


Fig. 1. Conceptual layout for an ERL injector coupled to the APS storage ring.

As we will see, the beam brightness will degrade as the beam circulates in the ring. Hence, for ultimate performance, single-turn operation is best. In this mode, the beam is extracted after one turn and sent back through the linac in the opposite direction. With continuous beam from the linac (or properly timed pulses), efficient energy recovery should be possible.

To avoid collisions between bunches, one can use cork-screw trajectories in the linac. For example, if the phase advance in the horizontal and vertical planes is the same, then the beams can be placed on cork-screw trajectories that never intersect. Another possibility is to spoil the emittance of the returning beam so that it is much larger than the primary beam. This might be done with a thin foil, provided power deposition is manageable. These are merely suggestions and have not been verified through simulation.

The return arc shown in Figure 1 could in time be replaced with a second

ring, which would double the number of possible beamlines.

A primary concern in this proposal is corruption of the beam quality by coherent synchrotron radiation (CSR), which has been found to have significant negative impacts in other projects [3]. Since the beam quality will be degraded in passing through the first ring, users on the second ring would not enjoy quite the same brightness as those on the first. It is possible that the new ring could be designed to better preserve the beam brightness than is possible with the existing APS ring. Hence, it would probably make more sense to inject first into the new ring and then into the existing ring.

In this paper, we look only at the beam degradation for the single-ring concept using the existing APS ring. Lacking a simulation input or design for the injector and linac, we have simply assumed some plausible beam properties: charge per bunch of order 100 pC, rms bunch length of order $50 \mu\text{m}$ (170 fs), normalized emittance of $1 \mu\text{m}$ in both planes, and rms energy spread of 0.01%. We have also assumed that the beam is Gaussian, which is almost certainly incorrect if the beam is delivered by an rf photoinjector, as seems most likely. It is known [4] that the details of the phase space are important in predicting CSR effects. As a result, the computations shown here should be taken as providing a lower bound on the beam quality.

2 Simulation Methods

In this section, we discuss details of simulation methods, including methods of simulating CSR and other effects. Simulations were performed with the code `elegant` [5]. Since we are primarily interested in beam behavior over one or a few turns, we have used element-by-element second-order matrix tracking. An exception is the dipoles and drift spaces, where we use elements that incorporate coherent and (in dipoles) incoherent synchrotron radiation effects.

The CSR algorithm used by `elegant` was described in [6]. In the modeling for this paper, each 3.05-m-long dipole is split into 20 pieces. Hence, the CSR “wake” is computed 20 times in each dipole. The transport from the end of one slice to the end of the next is accomplished with a fourth-order Ruth integrator [7].

While CSR is of course only emitted when the beam is inside the dipole, radiation from the end of each dipole propagates with the beam and continues to modify the energy distribution. The algorithm described in [6] was updated to improve the modeling of CSR in drift spaces, which is invoked with the CSRDRIFT element. The new model is based on a newly-derived expression

[8] for the CSR wake in drift spaces, whereas the original models were largely heuristic. Outside of dipoles, the effects of the CSR wake on particle motion is largely confined to the longitudinal plane. Using this approximation, `elegant`'s new model also includes CSR effects inside quadrupoles and sextupoles that are bracketed by CSRDRIFT elements. To implement this, we simply back-drift the beam to the position of the beginning of the multipole, then forward-drift with CSR effects back to the exit of the multipole.

In the simulations reported here, drift spaces were split into 5-cm segments. The relatively small step size ensures that the decay of the CSR field is properly modeled.

`elegant` allows simulation of CSR using either a transient or steady-state algorithm. Choosing the appropriate algorithm depends on the distance between dipoles and the so-called ‘‘overtaking length,’’ which characterizes the distance required for CSR to develop when the beam enters a dipole and fall off when it exits. The expression $L_0 = (24\rho^2\sigma_z)^{\frac{1}{3}}$ [9] involves the dipole radius ρ and the bunch length σ_z . Assuming $\sigma_z = 50\mu\text{m}$ and taking the value $\rho = 38\text{ m}$ for the APS dipoles, we obtain $L_0 = 1.2\text{m}$. This is much smaller than the distance between adjacent dipoles. Hence, the transient CSR model is appropriate for APS simulations.

Although `elegant` simulates only unshielded CSR, it is advisable to check whether this is a good approximation. The required chamber height to fully shield CSR [10] at wavelengths longer than σ_z is $0.2(\sigma_z^2\rho)^{\frac{1}{3}}$. The numerical value is 0.9 mm, which is much smaller than the 40-mm chamber gap in the dipoles. Hence, there is no shielding of CSR, and `elegant`'s model is acceptable.

Incoherent synchrotron radiation in the dipoles is modeled by adding random values to macroparticle momentum offsets at the end of each dipole slice. The change in the variance of the beam's momentum spread after one slice is [11]

$$\Delta\sigma_\delta^2 = 1.44 \times 10^{-27} \frac{\gamma^5 \theta}{\rho^2}, \quad (1)$$

where γ is the relativistic factor, θ is the bending angle of the slice, and ρ is the bending radius. Hence, we simply add to the δ value for each macroparticle random deviates with Gaussian parameter $\sqrt{\Delta\sigma_\delta^2}$. In addition, the classical synchrotron radiation loss must be included for each particle.

Noise is a particular problem with CSR simulations because CSR tends to amplify density spikes, which is the origin of the microbunching instability observed in simulations of linacs with multiple bunch compressors [3]. Hence, use of a large number of particles is indicated, as is careful choice of the

number of bins and parameters for smoothing. Based on prior experience with simulations for the Linac Coherent Light Source, we used 600 bins and a ± 1 bin Savitzky-Golay smoothing filter. Comparison of tracking with 100,000 and 1 million particles showed little difference in rms beam properties, but some differences in detailed beam distributions. To be conservative, we have used 1 million particles in all work presented here.

3 Choice of Lattice

We simulated the behavior of a high-brightness beam in the APS ring for three lattices:

- Lattice “LE”: A low-emittance lattice [12], which has a nominal emittance of 2.5 nm and an effective emittance of 3.1 nm. This lattice has dispersion of about 0.17 m in the straight sections. The lattice is very similar to the one presently used for APS operations. The x and y tunes are 36.26 and 19.36, respectively, which differs slightly from the tunes actually used for operations.
- Lattice “ZD”: high-emittance lattice with zero dispersion in the straight sections. The emittance is 7.7 nm, with x and y tunes of 35.25 and 19.35, respectively. Prior to the advent of top-up, this was the standard operating lattice for APS [13].
- Lattice “ISO”: An isochronous lattice with large emittance and dispersion in the straight sections. This might prove useful for larger energy spread beams, but has a very large equilibrium emittance of 25 nm. Unfortunately, in a double-bend system one cannot have a low-emittance isochronous lattice. The x and y tunes are 32.09 and 19.61, respectively.

One might anticipate that the LE lattice will have the least emittance growth due to both incoherent synchrotron radiation (ISR) and CSR. The equilibrium emittance is proportional to the well-known H function [14], which is smallest in this lattice. Differences in energy losses among particles in a bunch result in more emittance growth when H is large. The source of the energy loss variation may be quantum effects (as in ISR) or wake-like effects (as in CSR). Although these are expected to have similar effects, there are differences. For example, ISR happens uniformly along the dipole, while CSR must build up as the beam travels through the dipole.

Figures 2 through 4 show the energy spread, bunch length, and emittance vs distance in the presence of ISR but in the absence of CSR for the three lattices. These figures and all subsequent figures show the beam properties at the centers of the insertion device straights only. The ISO lattice is clearly much worse than the others in terms of emittance and better in terms of bunch

length, neither of which is surprising. The ZD lattice is slightly better than the LE lattice but shows more rapid growth. This can be understood by noting two factors. First, the emittances shown are effective emittances, which include beam size due to energy spread. Since the LE lattice has non-zero linear dispersion in the straight sections, it starts out with a larger effective emittance. In addition, increasing energy spread inflates the effective emittance directly. However, the effects of differential energy losses on emittance are stronger in the ZD lattice than in the LE lattice, due to H being larger. This results in the more rapid emittance growth in the ZD lattice. If one examines the “corrected” emittance, i.e., the emittance with the dispersion contribution eliminated, the LE lattice looks better than the ZD lattice.

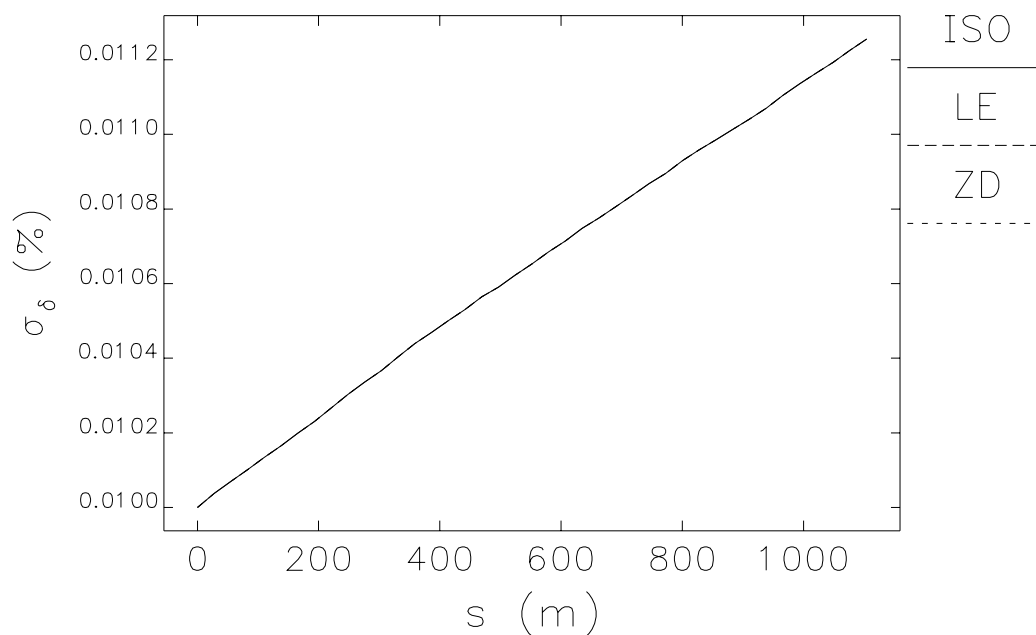


Fig. 2. Rms momentum spread as a function of distance in the APS for the three lattices, with ISR only. The results in this case are identical for all lattices.

Figures 5 through 7 show the energy spread, bunch length, and emittance vs distance in the presence of ISR and CSR. The energy spread results are very similar for the various lattices. This is expected, since *elegant*’s CSR algorithm is a line-charge model. This means that differences in energy spread evolution can only result from differences in bunch length evolution. We see from Figure 6 that there are only relatively small differences in the bunch lengths among the lattices. Not surprisingly, the ISO lattice is still best at maintaining a fixed bunch length. The ZD and LE lattices show an initial dip in bunch length, which results from the fact that CSR accelerates the head of the bunch and decelerates the tail. When combined with the positive momentum compaction of the lattice, the head of the bunch falls back while the

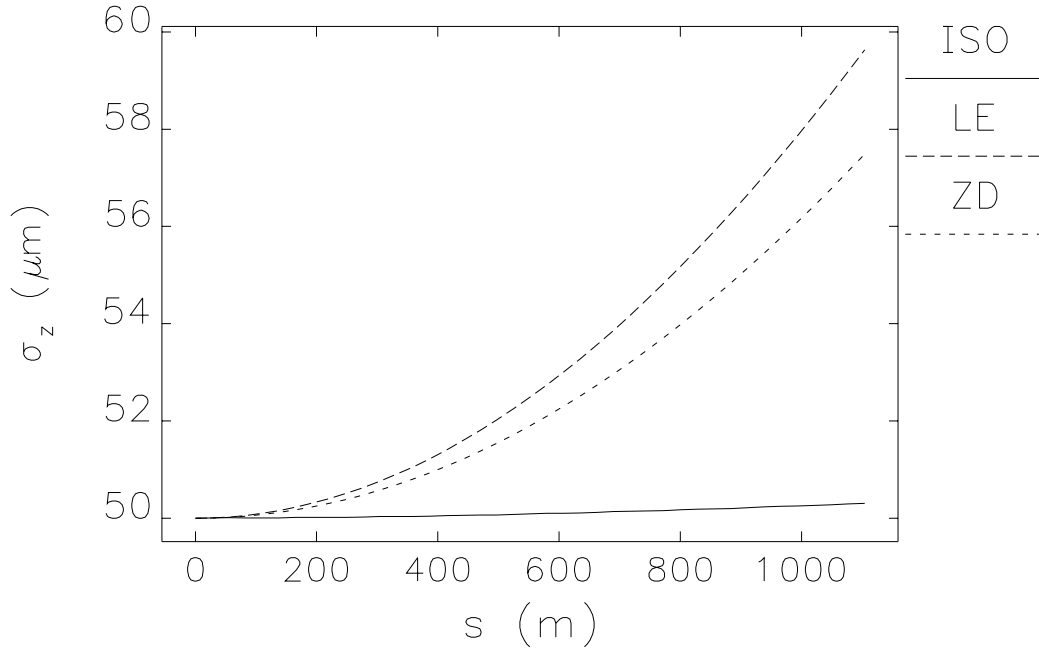


Fig. 3. Rms bunch length as a function of distance in the APS for the three lattices, with ISR only.

tail moves forward. At some point, the bunch gets over-compressed and starts to lengthen again. The ZD lattice has 15% smaller momentum compaction, so the minimum comes later and the increase is likewise delayed.

The difference in effective emittance between the ZD and LE lattices is surprisingly large. The ZD lattice shows very little additional emittance growth due to CSR, which is quite surprising given that the energy spread growth is much larger than in the case with ISR only. In contrast, the emittance increase for the LE lattice with CSR is ten times as great as the emittance increase with ISR only. Since H is larger in the ZD lattice, we conclude that the large emittance increase seen in the LE lattice is a result of the dispersion in the straight sections. Just as in the case with ISR only, if one examines the corrected emittance, the LE lattice looks better than the ZD lattice. However, x-ray brightness is related to the effective emittance. Since the ZD lattice is clearly better in this regard, all subsequent simulations use this lattice only.

Standard undulators in the APS have period lengths of 2.7 to 3.3 cm and are as long as 2.4 m. A superconducting device with period of 1.0 cm is contemplated [13] and might be as long as 4.8 m (the limit for APS straight sections). Such a device would have 480 periods and hence provide a spectral bandwidth [15] of about 0.2%. This is much larger than the energy spread seen in the simulations, and hence the energy spread per se is not a problem.

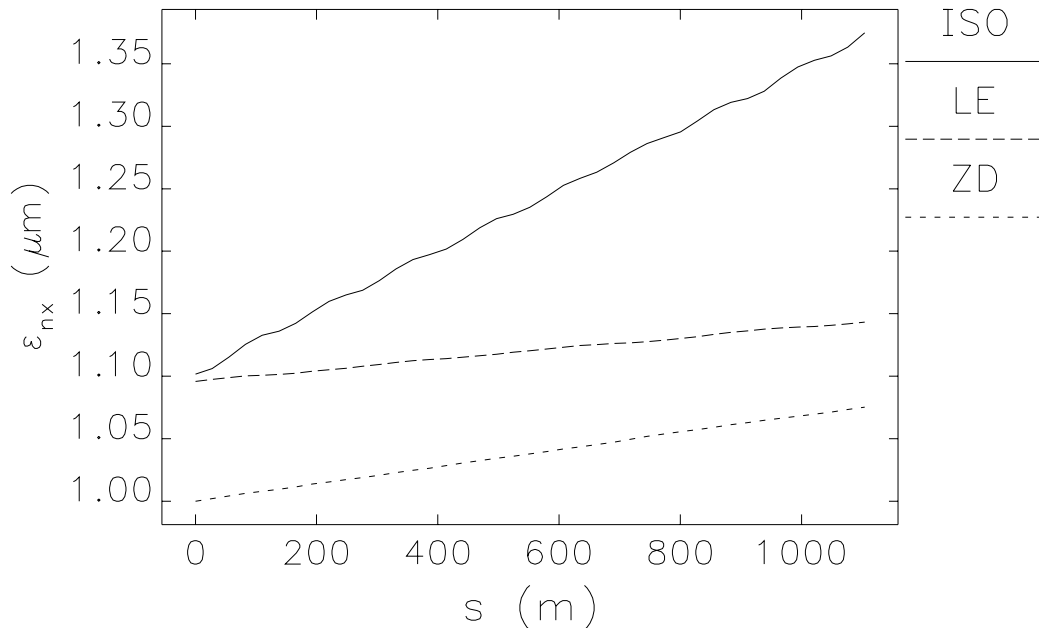


Fig. 4. Rms normalized effective emittance as a function of distance in the APS for the three lattices, with ISR only.

4 CSR Effects for the Zero-Dispersion Lattice

The evolution of the longitudinal phase space, shown in Figure 8, exhibits several interesting features. Ignoring the average energy loss of the whole bunch, we initially see a classic CSR-wake shape, where the head of the bunch is accelerated while the center and tail are decelerated. Due to the momentum compaction of the lattice, the head falls back and the tail moves forward, creating a region of higher current near the center of the bunch. This leads to even stronger CSR effects, resulting in a folded longitudinal distribution and appearance of charge clumps. These are reminiscent of effects seen in experiments [16] and also of the microbunching instability predicted by bunch compressor simulations [3]. It seems likely that if the initial phase space were not Gaussian, much more serious effects would arise, including the microbunching instability.

Next, we examined the variation in emittance growth as the charge in the beam is varied. Figure 9 shows the results at the end of the turn. The peak brightness is proportional to $Q/(\epsilon_{nx}\epsilon_{ny}\sigma_z)$, where Q is the charge, ϵ_{nx} and ϵ_{ny} are respectively the normalized horizontal and vertical emittance, and σ_z is the bunch length. This quantity peaks at $Q = 100$ pC, falling by more than 50% for 200 pC. Hence, we'll concentrate on the 100-pC case.

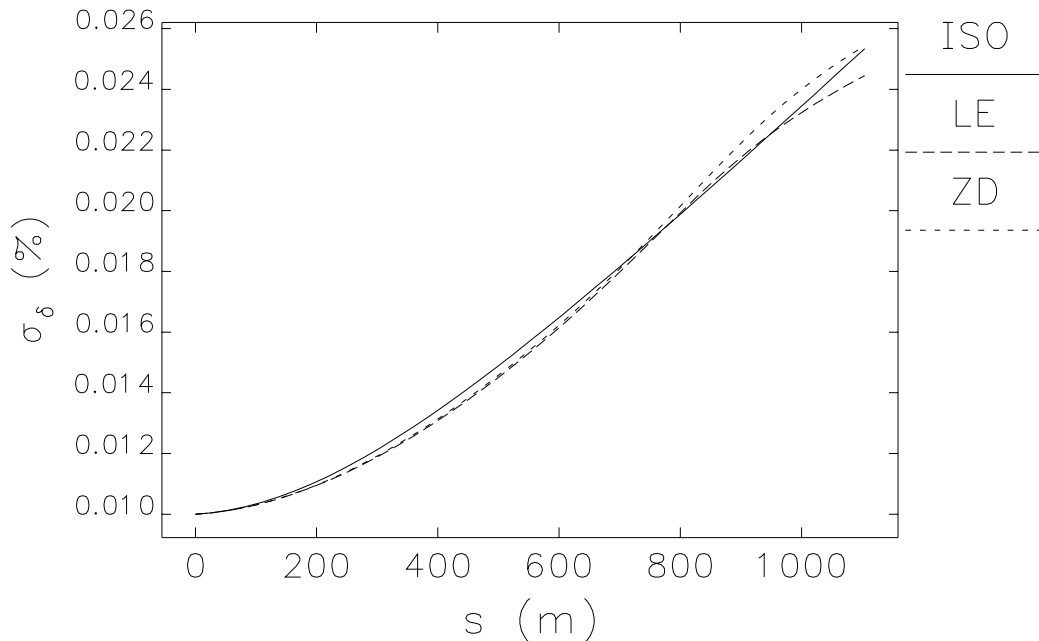


Fig. 5. Rms momentum spread as a function of distance in the APS for the three lattices, with ISR and CSR. The results in this case are identical for all lattices.

We used the program `sddsbrightness` [17] to compute brightness curves for the beam at the end of a turn for the ZD lattice, for a standard APS “undulator A,” which has a 3.3-cm period and a length of 2.4 m. Figure 10 shows a comparison of average brightness for the ERL beam to the present APS at 100 mA and 1% coupling. We assumed the ERL provided an average current of 100 mA. Also shown is a hypothetical case with 300 mA and 0.3% coupling. This case is not far-fetched, given that we’ve stored 225 mA in the APS and also (separately) run with 0.3% coupling. This comparison indicates that the ERL option is not impressive in terms of average brightness.

This may be surprising given that the assumed emittance for the ERL is 73 pm, much smaller than the effective APS equilibrium emittance of 3.1. However, the APS vertical emittance is 25 pm during normal operations, which is nearly diffraction limited for 1 Å radiation. The ERL beam with equal emittances in both planes is actually worse in the vertical plane than what APS normally uses now. Hence, with the ERL option we gain from the decrease in horizontal emittance but lose in the vertical plane.

An attractive feature of the ERL option is the short bunch length, which promises higher peak brightness. If we stored 300 mA in APS in 24 bunches, we would expect an rms bunch length of about 15 mm and a peak current of about 300 A. (This corresponds to 12.5 mA in a single bunch, which has been achieved in APS.) In the ERL example used here, the bunch length is

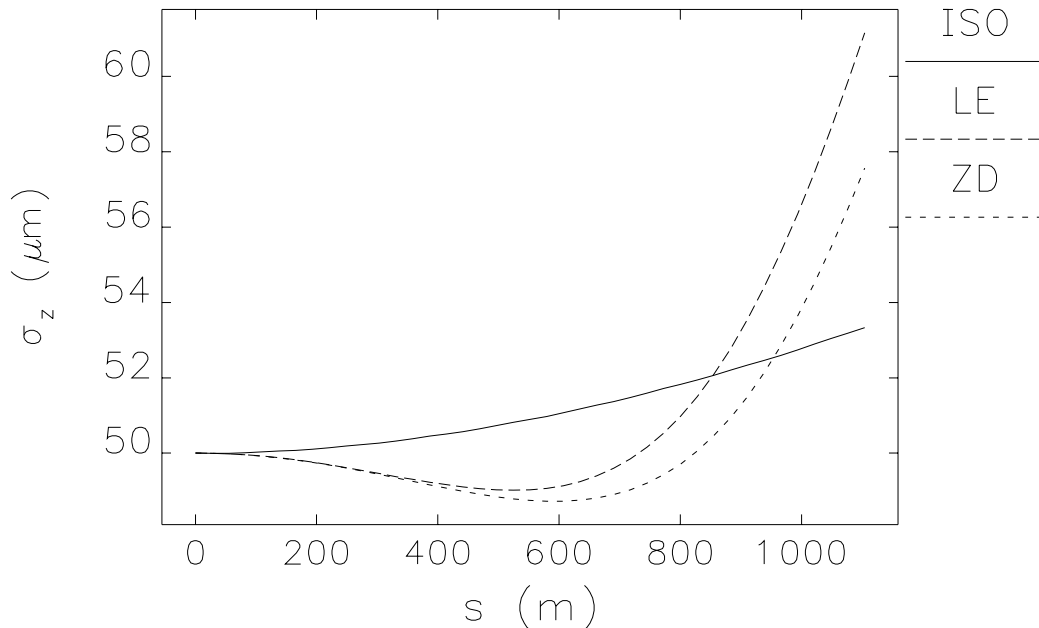


Fig. 6. Rms bunch length as a function of distance in the APS for the three lattices, with ISR and CSR.

50 μm and the charge is 100 pC, giving 240 A. Hence, we do not expect an advantage in peak brightness from the ERL relative to APS at 300 mA and low coupling.

For experiments that require a short probe pulse, this comparison is not relevant and the ERL option apparently has a decisive advantage. However, it is unclear whether the 1-GHz repetition rate required to obtain an average current of 100 mA is suitable for a significant class of timing experiments. In contrast, the standard 24 bunch pattern in APS provides 150-ns spacing of pulses that can be used by timing experiments. Other fill modes provide even larger spacing. When combined with crab-cavity-based schemes for x-ray compression [18,19] it may well be that a traditional storage-ring-based approach is advantageous for many timing experiments.

5 Conclusion

We have examined through simulation the potential performance of injecting a high-brightness beam from an Energy Recovery Linac into the APS storage ring. We find that beam properties are best preserved by using a lattice with zero dispersion in the straight sections, even though this lattice does not have the smallest H function. We find that for nominal beam parameters of

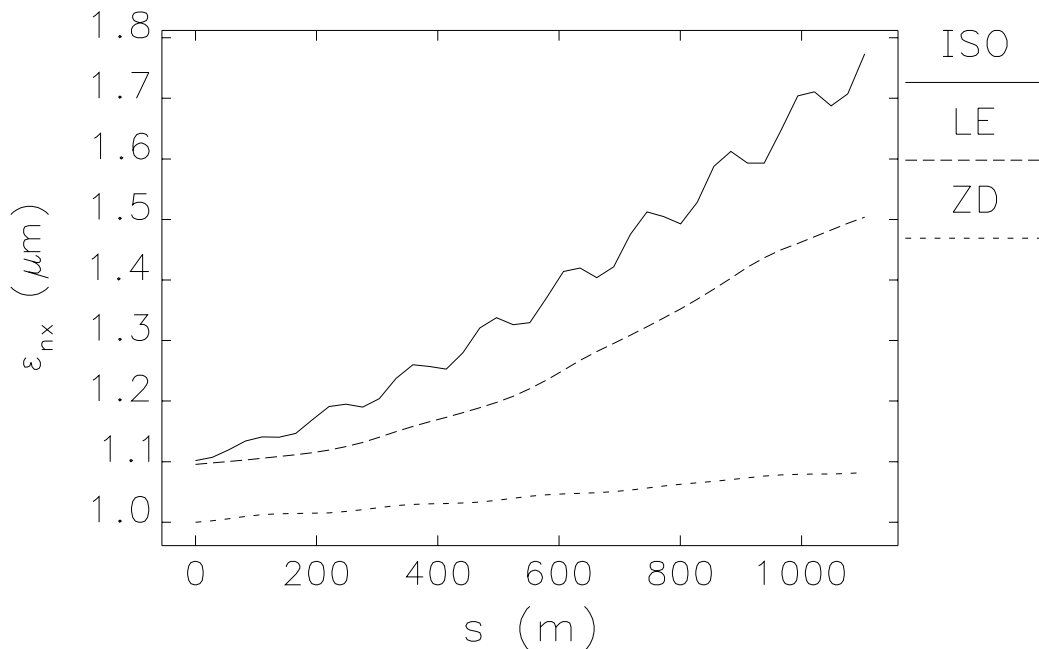


Fig. 7. Rms normalized effective emittance as a function of distance in the APS for the three lattices, with ISR and CSR.

100-mA average current, 1- μm normalized emittance, 0.01% rms momentum spread, and 100-pC charge, the average brightness is higher than present-day APS operation by just under a factor of ten. Reasonable extrapolation of APS operation parameters leads to a negligible advantage for the ERL. Similarly, literal calculation of the peak brightness for the ERL and extrapolated APS performance shows no advantage for the ERL. Although the ERL clearly produces much shorter electron pulses, a storage ring has more flexible timing and, when combined with x-ray compression techniques, may prove competitive and cost effective.

References

- [1] L. Emery and M. Borland, "Possible Long-Term Improvements to the Advanced Photon Source," Proc. of the 2003 PAC, Portland, Oregon, 256 (2003).
- [2] J. B. Murphy, "Energy Recovery Linac Light Sources: An Overview," Proc. of the 2003 PAC, Portland, Oregon, 176 (2003).
- [3] M. Borland, Y.-C. Chae, S. Milton, R. Soliday, V. Bharadwaj, P. Emma, P. Krejcik, C. Limborg, H.-D. Nuhn, and M. Woodley, "Start-to-End Jitter Simulations of the Linac Coherent Light Source," Proc. of the 2001 PAC, Chicago, Illinois, 2707 (2001).

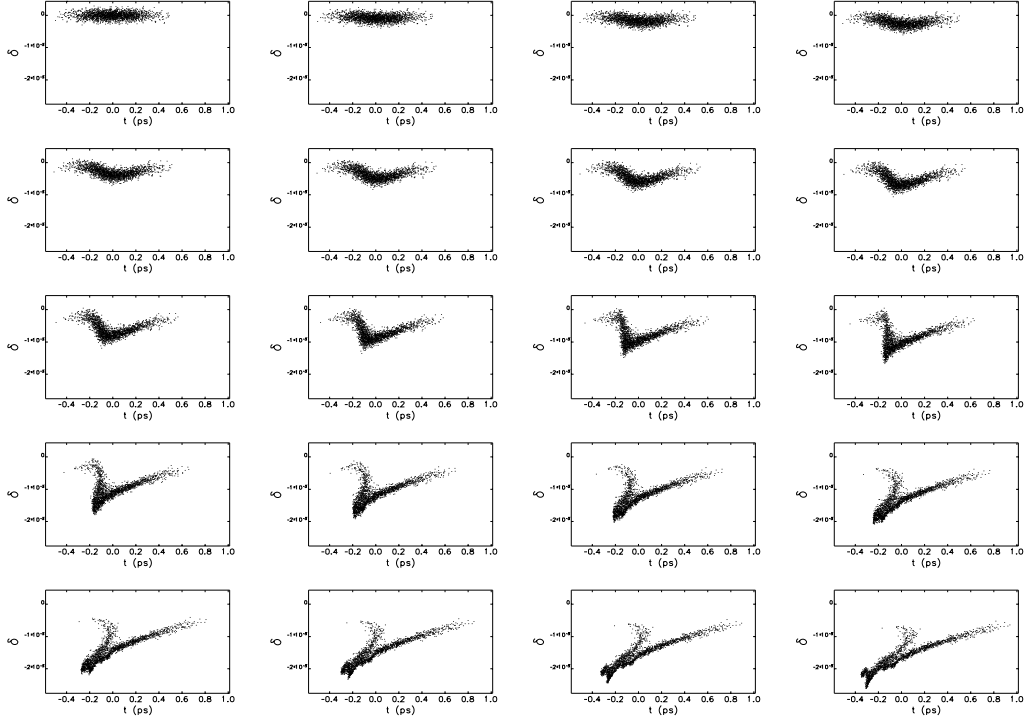


Fig. 8. Longitudinal phase space at the center of every other straight section for the ZD lattice, assuming 100 pC, 50- μ m initial rms bunch length, 0.01% initial rms momentum spread, and 1- μ m initial normalized emittance.

- [4] R. Li, “Analysis and Simulation of the Enhancement of the CSR Effects,” Proc. of the XX International Linac Conference, Monterey, California, 262 (2000).
- [5] M. Borland, “elegant: A Flexible SDDS-Compliant Code for Accelerator Simulation,” Advanced Photon Source Light Source Note LS-287, September 2000.
- [6] M. Borland, “Simple method for particle tracking with coherent synchrotron radiation,” Phys. Rev. ST Accel. Beams 4, 070701 (2001).
- [7] E. Forest, AIP Conference Proceedings 184 (1989) 1106-1136.
- [8] G. Stupakov and P. Emma (SLAC), “CSR wake for a short magnet in ultrarelativistic limit,” SLAC-PUB-9242, May 2002.
- [9] E. L. Saldin, E. A. Schneidmiller, and M. V. Yurkov, NIM A 398 (1997) 373.
- [10] M. Borland, “Coherent Synchrotron Radiation and Microbunching in Bunch Compressors,” Proc. of the XXI Linac Conference, Gyeongju, Korea, 11 (2002).
- [11] G. Leleux, P. Nghiem, and A. Tkatchenko, Proceedings of the 1991 PAC, May 6-9, 1991, San Francisco, California, 571 (1991).
- [12] L. Emery and M. Borland, “Upgrade Opportunities at the Advanced Photon Source Made Possible by Top-up Operations,” Proc. of the 2002 EPAC, Paris, France, 218 (2002).

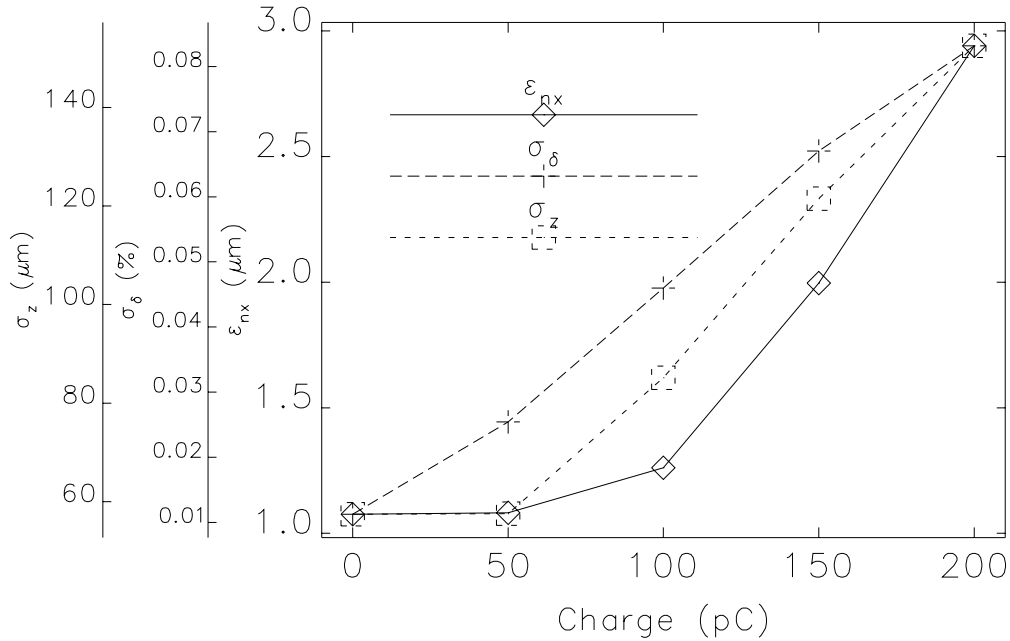


Fig. 9. Rms beam properties after one turn as a function of charge for the ZD lattice, assuming 100 pC, 50- μm initial rms bunch length, 0.01% initial rms momentum spread, and 1- μm initial normalized emittance.

- [13] L. Emery, M. Borland, R. Dejus, E. Gluskin, and E. Moog, “Progress and Prospects Toward Brightness Improvements at the Advanced Photon Source,” Proc. of the 2001 PAC, Chicago, Illinois, 2602 (2001).
- [14] R. H. Helm, M. J. Lee, P. L. Morton, and M. Sands, “Evaluation of Synchrotron Radiation Integrals,” SLAC-PUB-1193, March 1973.
- [15] H. Weidemann in *Handbook of Accelerator Physics and Engineering*, A. W. Chao and M. Tigner eds., Section 3.1.5, World Scientific (1999).
- [16] T. Limberg, Ph. Piot and E. A. Schneidmiller, “An analysis of longitudinal phase space fragmentation at the TESLA test facility,” NIM A 475 (2001) 353.
- [17] M. Borland, L. Emery, H. Shang, and R. Soliday, “SDDS-Based Software Tools for Accelerator Design,” Proc. of the 2003 PAC, 3461 (2003).
- [18] A. Zholents, P. Heimann, M. Zolotarev and J. Byrd, NIM A 425 (1999) 385-389.
- [19] M. Borland, “Simulation and analysis of using deflecting cavities to produce short x-ray pulses with the Advanced Photon Source,” submitted to Phys. Rev. ST Accel. Beams.

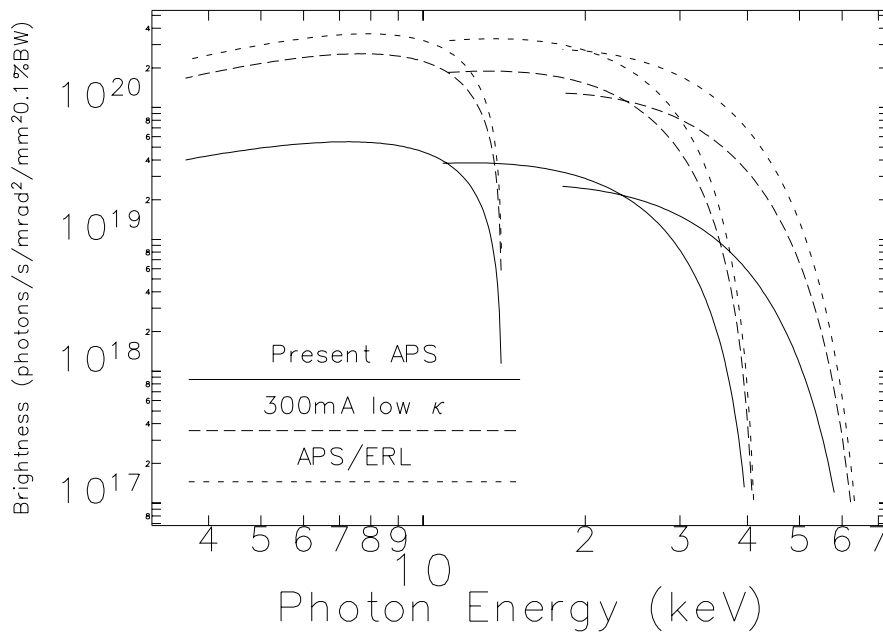


Fig. 10. Average brightness for present APS operation, APS operation with high current and low coupling, and APS operation with 100-mA ERL injection. A standard APS undulator with a period of 3.3 cm and a total length of 2.4 m is assumed.